https://doi.org/10.5194/wcd-2022-59
Preprint. Discussion started: 28 November 2022

Weather and Climate Dynamics Discussions
Open Access
EGU

Transient Anticyclonic Eddies and Their Relationship to Atmospheric Block Persistence

Charlie C. Suitters[1], Oscar Martínez-Alvarado[1,2], Kevin I. Hodges[1,2], Reinhard K. H. Schiemann[1,2], and Duncan Ackerley[3]

[1]Department of Meteorology, University of Reading, Reading, United Kingdom
[2]National Centre for Atmospheric Science (NCAS), University of Reading, Reading, United Kingdom
[3]Met Office, Exeter, United Kingdom

Correspondence: Charlie Suitters (c.c.suitters@pgr.reading.ac.uk)

Abstract. Atmospheric blocking is a circulation pattern that describes the presence of large-scale, persistent anticyclones, which have the potential to bring severe impacts at the surface. However, the dynamical behaviour of blocks is still not fully understood. For example, the factors that determine the persistence of blocking events are not clear. In this study, the relationship between blocks and smaller-scale transient anticyclonic eddies is examined, with a particular focus on the impact of transients on the persistence of a block. Analysis is performed in two areas: the Euro-Atlantic and North Pacific, which are locations with both high blocking frequency and potential for severe impacts. Geopotential height anomalies at 500 hPa are used to identify blocking events and the anticyclonic transient eddies. This allows for a Eulerian definition of blocking, as well as a Lagrangian perspective on the eddies. It is found that anticyclonic eddies experience a northward acceleration prior to entering a block, which is indicative of ridge-building ahead of a block, but could also potentially provide evidence for the previously-proposed Selective Absorption Mechanism for block maintenance. A general pattern is found whereby longer blocks interact with more anticyclonic transients than less persistent blocks at all times of year. This effect is strongest in winter and weakest in summer, which agrees with the fact that blocks are most persistent in winter and least persistent in summer. However, the strength of the anticyclonic eddy, measured by its maximum 500 hPa geopotential height anomaly, that interacts with a block generally has very little bearing on the persistence of a block, aside from a few cases.

1 Introduction

Extratropical atmospheric blocking is important due to the anomalous, and sometimes severe, weather conditions that are often observed at the surface. These conditions occur due to anomalously large and slow-moving high pressure systems characteristic of blocking weather patterns, which act to disrupt the climatological mid-latitude zonal flow, instead diverting it to the north and south (Rex, 1950).

A complete dynamical understanding of block formation, maintenance, and decay is still lacking. One of the main reasons for this is the difficulty in defining what constitutes a block (Woollings et al., 2018) due to the large array of synoptic conditions that can be described as "blocked". Compounding this issue further is the fact that there are numerous ways to define and detect a block in gridded datasets (Barriopedro et al., 2010; Woollings et al., 2018), and there is no one method that detects every

https://doi.org/10.5194/wcd-2022-59
Preprint. Discussion started: 28 November 2022

Weather and Climate Dynamics Discussions
Open Access
EGU

weather pattern that a synoptician would identify as a block. However, the overwhelming consensus is that blocking events are qualitatively described by their high surface pressure, persistence, large spatial area, and quasi-stationarity (Rex, 1950), with blocks typically lasting 1-2 weeks (e.g., Woollings et al., 2018; Lupo, 2021; Kautz et al., 2022).

With these characteristics in mind, previous studies have been able to identify a range of mechanisms that are important for blocking, with most of the focus on block formation processes. Large-scale wave dynamics are a principal way in which blocks can form, for example through a simple stationary ridge in the planetary wave pattern (Legras and Ghil, 1985), constructive interference of waves with different scales (Austin, 1980; Shutts, 1983), or Rossby wave breaking (e.g., Altenhoff et al., 2008; Masato et al., 2012). Other processes important to block formation include rapid cyclogenesis (Colucci, 1985; Nakamura and Huang, 2018) and diabatic heating (Pfahl et al., 2015; Lenggenhager and Martius, 2020; Zschenderlein et al., 2020). The relative importance of these mechanisms varies by location (Miller and Wang, 2022), and can even vary within a region (Drouard and Woollings, 2018), which suggests that block formation is complex. More recently, there have been studies on the specific processes for block maintenance, in an attempt to explain why some blocks persist for longer than others. For example, Drouard et al. (2021) examined Northern Hemisphere (NH) blocks and concluded that the most important factor in determining block persistence was the direction of the Rossby wave breaking. Cyclonically-breaking blocks tend to be longer lived than blocks that form from anticyclonic wave breaking. However, their study assumes that all blocks can be classified by the direction and morphology of wave breaking, when in fact a blocking event can take many different shapes (e.g. ridge, omega, dipole/Rex, cyclonic and anticyclonic wave breaking) during its lifetime (e.g., Sousa et al., 2021).

It has long been known that there is a two-way interaction between blocking systems and smaller-scale synoptic transient eddies. Blocks cause synoptic eddies to slow down and stall, while these same eddies can enhance and maintain the block (e.g., Shutts, 1983; Mullen, 1987). One of the first studies to examine this relationship was that of Shutts (1983), where the Eddy-Straining Mechanism (ESM) was developed. In the ESM theory, diffluent flow immediately upstream of a dipolar high-over-low block causes transient synoptic eddies to become stretched and split into a poleward and equatorward component. Then, on the poleward side of the block, anticyclonic vorticity forcing induced by the eddies reinforces the blocking high; meanwhile the blocking low is maintained by the cyclonic vorticity forcing of the eddies on the equatorward side. The ESM can also explain how blocks are prevented from downstream advection by the background westerlies (Mullen, 1987), but does not consider how eddies of opposing polarities interact with the block. The ESM also only assumes a meridional dipolar structure (akin to a Rex block) and therefore cannot be applied to all blocking events.

Yamazaki and Itoh (2009, 2013a, b) proposed a more general process for block maintenance called the Selective Absorption Mechanism (SAM), which is valid for blocks of all shapes, in all locations and at all times of year. The SAM assumes that blocks are large-scale areas of anticyclonic potential vorticity (PV) that attract smaller synoptic-scale anticyclonic eddies and repel synoptic-scale cyclonic eddies through differential vorticity advection. The attraction and absorption of the negative PV anomaly associated with the anticyclonic eddies reinforces the block, allowing it to persist for longer. The SAM also explains the reinforcement of the cyclonic systems associated with omega or dipole blocking too, if present, as these selectively attract synoptic lows and repel synoptic highs. Therefore, the presence of transient eddies is crucial to the maintenance of a blocking event, though there has been very little work to date on the exact quantitative relationship between eddies and blocks.

https://doi.org/10.5194/wcd-2022-59
Preprint. Discussion started: 28 November 2022

Specifically, a study into the amount to which synoptic eddies are absorbed by blocks, or the magnitude of the eddies that contribute towards blocking, and how these eddy characteristics affect the persistence of a block is lacking.

All studies of blocking require some form of objective blocking definition. A vast selection of techniques have previously been proposed which include weather regime classification (Vautard, 1990; Grams et al., 2017) or self-organising maps (Thomas et al., 2021); field reversals in meridional geopotential height (Lejenäs and Økland, 1983; Tibaldi and Molteni, 1990; Scherrer et al., 2006) and potential temperature on the dynamical tropopause (Pelly and Hoskins, 2003; Tyrlis and Hoskins, 2008); and anomalies in geopotential height (Charney et al., 1981; Shukla and Mo, 1983; Schwierz et al., 2004; Liu et al., 2018; Schiemann et al., 2020). The diversity in blocking metrics arises from the fact that there is no perfect way to detect blocking events, and each method has been designed with a specific purpose in mind. The most common blocking indices have well-documented strengths and drawbacks, as highlighted in Barriopedro et al. (2010). A method that detects both blocks and their contributing anticyclonic transient features has not yet been developed and thus this current study calls for another detection method that is able to capture both.

A common way to detect and follow meteorological features is through objective feature tracking. This approach is common when studying cyclonic systems (e.g., Hodges et al., 2011; Catto et al., 2011; Sainsbury et al., 2020; Priestley et al., 2020), and a few studies have employed similar techniques for anticyclones (e.g., winter anticyclones affecting China in Chen et al. (2014); NH winter anticyclones in Ioannidou and Yau (2008); a global anticyclone climatology in Pepler et al. (2019)). Recent work by Liu et al. (2018) performed feature tracking on persistent 500 hPa geopotential height (Z500) anomalies to build a climatology of where these persistent anomalies (analogous to blocks) occur. However, these previous studies all focused on large scale anticyclones or blocks themselves, rather than the smaller anticyclonic (AC) eddies that help form and maintain them. This current study aims to identify and track these AC eddies that contribute towards blocking. Once identified, the relationship between transient AC eddies and block persistence will be established in terms of both (i) how the number of eddies contributing towards a block affects its persistence, and (ii) how eddy intensity, size, and speed affects block persistence. This analysis will be performed for both the Euro-Atlantic and North Pacific regions, with a focus on winter and summer.

The paper is structured as follows. Section 2 describes the data used in this work, and also discusses how AC eddies and blocks are defined in this study. Section 3 demonstrates how AC eddies can interact with a block event with a short case study. Section 4.1 describes the spatial distribution of blocks, while Sect. 4.2 describes the persistence distribution of blocks. The relationship between block persistence and the number of contributing AC eddies is discussed in Sect. 5.1, while Sects. 5.2 and 5.3 show how the strength of AC eddies varies in time for all blocks, and blocks of different lengths respectively. Finally, the work is summarised in Sect. 6.

2 Data and Methods

2.1 Data

The data used in this study are taken from the European Centre for Medium-Range Weather Forecasts (ECMWF) 5th generation reanalysis (ERA5) (Hersbach et al., 2020). The blocking index and feature-tracking are based on analysis of 6-hourly Z500

https://doi.org/10.5194/wcd-2022-59
Preprint. Discussion started: 28 November 2022

data from 1 March 1979 – November 2021 with an F128 grid resolution. This is a regular Gaussian grid, with a grid size of approximately 0.7°, and is coarser than the full ERA5 resolution of 0.25°. Experiments were performed at different resolutions and the conclusions made did not change appreciably. Thus, the F128 was chosen in the interest of computational speed. Data are additionally separated into the traditional meteorological seasons for further analysis in this work: winter (December, January, February; DJF), spring (March, April, May; MAM), summer (June, July, August; JJA), and autumn (September, October, November; SON).

2.2 Anticyclonic Eddy Definition

2.2.1 Anticyclonic Anomalies

Despite the large array of existing block detection methods (discussed in Sect. 1), the majority have some drawbacks that would make a climatological study of the AC eddies that contribute to blocking difficult. For example, some methods require a certain aspect of subjectivity, unrealistically small blocks, or even fail to detect blocks of a certain shape (Barriopedro et al., 2010). These issues are particularly prominent for Z500 reversal-based techniques. It is also desirable to identify the AC eddies and blocks at the same time, and synoptic-scale eddies are unlikely to produce a marked reversal in the meridional Z500 gradient. Thus, a Z500 anomaly-based detection method was pursued.

In this study, blocks and anticyclonic eddies are defined as regions with a large positive Z500 anomaly from the zonal mean. The algorithm from Liu et al. (2018) is adapted in this study, to also consider the climatological wave patterns. The Z500 anomalies used to define the transients and the blocks (Z'_*) are calculated at each grid point (with longitude λ and latitude ϕ) and are given by:

$$Z'_*(\lambda,\phi) = Z_*(\lambda,\phi) - \overline{Z_*}(\lambda,\phi) \tag{1}$$

where $Z_*(\lambda,\phi)$ is the instantaneous Z500 anomaly from the instantaneous zonal mean, and $\overline{Z_*}(\lambda,\phi)$ is the climatological (1979-2021) monthly zonal mean Z500, where three-month smoothing has been applied.

At this stage, the importance of accounting for the climatological wave pattern ($\overline{Z_*}$) is noted. Figure 1 shows the monthly climatological $\overline{Z_*}$ pattern for all 12 months of the year. A stationary wave train is evident for much of the autumn, winter, and spring months, with the largest anomalies in winter. These anomalies are also consistent with the shape of the climatological North Atlantic and North Pacific storm tracks (Hoskins and Hodges, 2019). Climatological ridging occurs over a large band from the central North Atlantic to central Eurasia, with a deep trough to the east of this centred over northern Japan. Over the eastern North Pacific and western North America, a smaller and less intense region of ridging is present, followed by another trough downstream over the northeast of the continent. In summer, the same pattern manifests but is much weaker. Without considering $\overline{Z_*}$ when calculating the blocking index, regions of climatological ridging would show a large positive blocking frequency bias due to the high Z_*. Similarly, block frequency bias would be largely negative over regions of climatological troughing. In the work that follows, blocks are therefore considered to be anomalous circulation patterns within the climatological ridges and troughs, rather than simple anomalies in the zonal flow pattern.

https://doi.org/10.5194/wcd-2022-59
Preprint. Discussion started: 28 November 2022

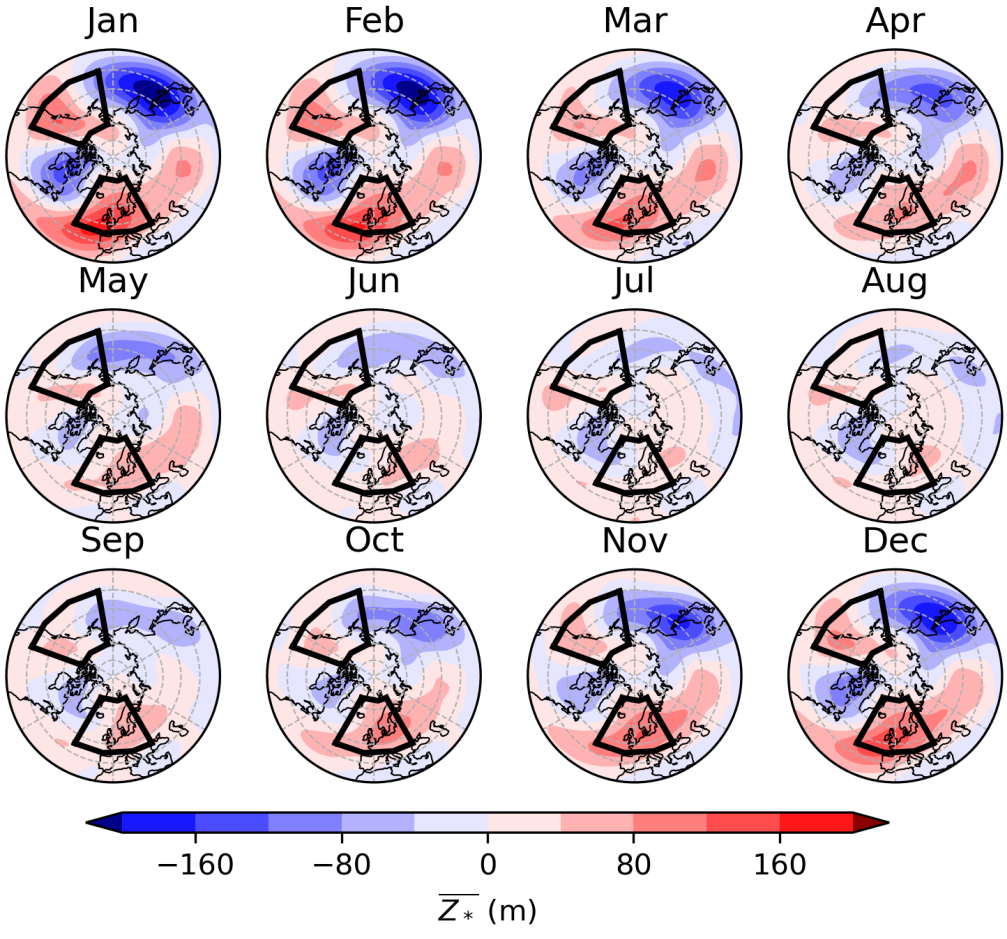

Figure 1. Monthly climatological $\overline{Z_*}$ from 1979–2021 (in metres) for January–December (shading). Also shown are the ATL and PAC regions (black boxes) used in this study (defined in Sect. 2.3).

2.2.2 Anticyclonic Eddy Tracking

125 The 6-hourly positive Z'_* centres are followed using an objective feature-based tracking algorithm (TRACK; Hodges (1994, 1995, 1999)). Tracking begins when $Z'_* \geq 60$ m and stops when the strength of an eddy goes below this value. This low threshold allows for the path of the eddy to be tracked both before and after it is part of a block, providing insights into the life cycle of anticyclonic transient eddies that contribute towards blocks. The tracks of the eddies are then filtered according to whether they are considered to contribute to a blocking event or not (Sect. 2.4).

https://doi.org/10.5194/wcd-2022-59
Preprint. Discussion started: 28 November 2022

Weather and Climate Dynamics Discussions
Open Access
EGU

2.3 Blocking Index and Sector Blocking Definition

The Z'_* field is also used to calculate a Eulerian blocking index at each grid point every six hours. For a grid point to be blocked, Z'_* must exceed 100 m for five or more consecutive days. This results in a 43-year time series at each grid point determining the periods in which the Z'_* magnitude and persistence threshold are met for blocking. Finally, sector blocking events (hereafter "blocks") are defined to occur when the area of blocked grid points inside a domain exceeds 1×10^6 km^2 (around 10% of either domain). This is only half the minimum size criterion imposed in Schiemann et al. (2020) for the ANOM index, but sensitivity tests showed that the results presented in this study are not dependent on the minimum size threshold (not shown). Sector blocking events are determined for two regions: the Euro-Atlantic (hereafter "ATL", 30° W–30° E, 45° N–75° N) and the North Pacific/northwest North America (hereafter "PAC", 170° W–110° W, 40° N–70° N). The domains are shown by black boxes in Fig. 1. These domains are both 60 degrees longitude wide, which is similar to the domain width used in Pelly and Hoskins (2003) but 15 degrees larger than in Tyrlis and Hoskins (2008). However, the ATL and PAC domains were defined to be this wide in this study to account for the moving position of the climatological blocking maxima in these regions in different seasons. This was done while also minimising the chance that more than one blocking event is captured in the domain at the same time. The regions were also designed to align with large population centres with relatively large climatological blocking frequencies, such that the blocks analysed in this study have the potential to cause widespread impacts. Further sensitivity tests were performed where the domain size and position were adjusted (also not shown) and the general conclusions drawn did not change.

2.4 Attributing Eddy Tracks to Blocks

A final step is required to filter some of the Z'_* tracks such that only those that are considered to be AC eddies are included for further analysis. Three scenarios where the tracks and blocks overlap are considered to be contributing eddies (Fig. 2):

- "Through" eddies (Track A in Fig. 2), where a Z'_* track starts and finishes outside a block, but travels through a group of blocked grid points somewhere in its lifetime.
- "Absorbed" eddies (Track B) where a Z'_* track starts outside and finishes inside a collection of blocked grid points.
- "Edge" eddies (Track C) that fluctuate between coinciding with blocked grid points, and outside a block. These tend to occur on the edge of a group of blocked grid points, or in the onset/decay phase of a block.

Anomaly tracks can also coincide in space and time with blocking events in two other ways, which will briefly be mentioned here. First, "internal" tracks are Z'_* tracks that predominantly (over 80% of the time) remain inside a block throughout their lifetime. These are normally very slow-moving features, which are representative of the movement of the blocking anticyclone centre. These tracks are therefore not considered to be AC eddies that contribute to blocking. Secondly, blocks can also occasionally produce "spawned" eddies, which are Z'_* tracks that start inside a blocked region and leave at some stage later in their lifetime. These cases are also not considered to be eddies that contribute to the block they spawn in, however they may go on to become an AC eddy associated with a different blocking event outside of their genesis region.

https://doi.org/10.5194/wcd-2022-59
Preprint. Discussion started: 28 November 2022

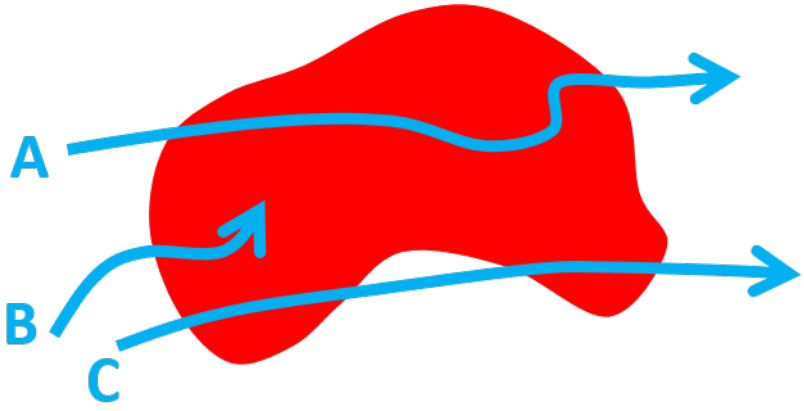

Figure 2. The three scenarios where AC tracks are considered to be contributing to blocking. Track A shows an eddy that passes through the block, Track B shows an eddy absorbed by the block, and Track C shows an eddy that fluctuates between coinciding with a block and not with a block. Tracks A, B and C are all considered to be AC eddies contributing to blocking.

3 Case Study of a Block and Transient Eddies

In this section, a case study is discussed to illustrate how transient eddies can both establish and maintain a blocking event. This event meets the sector blocking definition in the ATL region for 11.25 days, from 25 February–8 March 2011, and has a total of two AC eddies (with an additional two internal tracks and one spawned track). Figure 3 shows the Z'_* field and blocked points at 12 UTC for every day of the event. Additionally, all AC eddy, internal, and spawned tracks for this event are shown in each panel.

On 25 February, a ridge breaking in the far east of the domain gives rise to grid-point level blocking (Fig. 3a). At this stage, there is no Z'_* track in the domain, though one is present over the Scandinavian block just outside the ATL domain (not shown). By 26 February (Fig. 3b), a small AC eddy (dark blue line) originating from the mid-Atlantic can be seen approaching from the west as a low-amplitude ridge in the Z'_* field. This eddy enters the domain on 27 February (Fig. 3c) and this associated ridge amplifies, while the block situated in the east of the sector over Scandinavia remains in place. On 28 February (Fig. 3d), the western ridge breaks and connects to the Scandinavian block, resulting in many more blocked grid points in the domain, even in the west by this stage. Also on 28 February, the ATL block spawns an eddy (light blue line in Fig. 3) that travels towards the Ural Mountains until 3 March. A small internal track (medium blue line) is also present on the far eastern part of the domain, associated with a slight movement in the central anticyclone between 28 February and 1 March (so no yellow dot is shown). Meanwhile, another AC eddy has already begun travelling towards the block. This eddy orignated from the United States, and will eventually travel all the way to Japan, via the ATL block, travelling around 240 degrees longitude from start to end. At this early stage (28 February), this eddy is still fairly small, but over the next few days it grows in both size and amplitude as it connects to the ATL block (Fig. 3d-f). Another, more prominent internal track develops inside the block from 1–2 March.

https://doi.org/10.5194/wcd-2022-59
Preprint. Discussion started: 28 November 2022

Weather and Climate Dynamics Discussions
Open Access
EGU

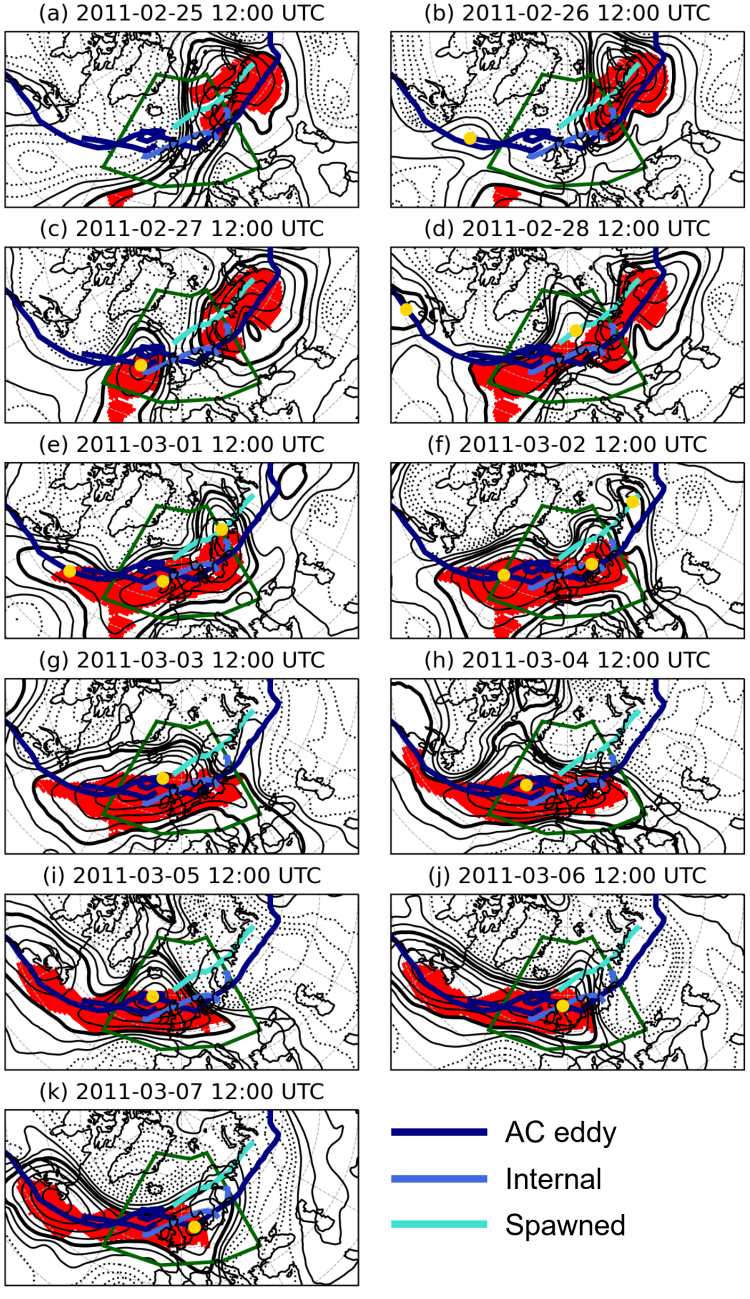

Figure 3. Blocked grid points (red shading) and Z'_* anomaly field (black contours at 50 m intervals; negative values dashed, 100 m line bold) at 12 UTC for each day of an ATL blocking event (the ATL region is depicted by the green box). AC eddy tracks (dark blue), internal tracks (medium blue) and spawned tracks (light blue) that coincide with this blocking event are also shown in each panel, with each track's position at the valid time shown by the yellow dot. Note that the small internal track on the eastern edge of the domain occurs between two 12 UTC time steps, so does not have a yellow dot in any panel.

https://doi.org/10.5194/wcd-2022-59
Preprint. Discussion started: 28 November 2022

Once inside the block, the Atlantic AC eddy slows down (as shown by the loop in its track from 3–5 March, Fig. 3g-i). On 6 and 7 March, the AC eddy begins to speed up again as it travels east towards Japan, and the ATL block slowly decays (Fig. 3j-k). Once the track leaves the ATL domain, very few grid points remain blocked and the block event finishes.

4 Northern Hemisphere Z'_* Index Blocking Climatology

4.1 Spatial Climatology

Before examining the transients that maintain blocks in the ATL and PAC domains, a climatology of NH blocking using the Z'_* (from Eq. 1) index is presented to motivate the selection of these two regions. Figure 4 shows the percentage of blocked days in winter, spring, summer, and autumn for the Northern Hemisphere. The spatial distribution of blocking frequency is consistent with many previous studies that utilise Z500 anomalies as a block detection algorithm (e.g., Barriopedro et al., 2010; Schiemann et al., 2017; Woollings et al., 2018). Blocking occurs most frequently in three regions: the Northeast Pacific/Northwest North America, Northeast Atlantic/Western Europe, and Scandianvia/Ural Mountains. The effect of considering the climatological stationary wave features ($\overline{Z_*}$) is noticeable here by comparing Fig. 4 with that of Liu et al. (2018) where $\overline{Z_*}$ is not considered (their Fig. 9). Climatological blocking frequencies as measured using the Z'_* index are 15–20 percentage points less frequent in the Pacific and Atlantic maxima than in Liu et al. (2018) (climatological frequency of 16% vs 30%).

Climatological blocking frequency also varies seasonally. Blocking is most frequent in winter and least frequent in summer, with spring and autumn having intermediate blocking frequencies. A few block detection methods instead find that summer contains the most blocked days and winter the fewest, for example when using a method that follows the jet stream (Barnes et al., 2012), or when classifying Euro-Atlantic circulation patterns through weather regimes (Büeler et al., 2021). However many methods agree with the result presented here that summer blocking is less frequent than winter blocking (e.g. Dole and Gordon, 1983; Barriopedro et al., 2010; Schiemann et al., 2017; Woollings et al., 2018). Although summer may anecdotally be more anticyclonic in the mid-latitudes than in the winter, summer blocks (Wiedenmann et al., 2002), and anticyclones more generally (Pepler et al., 2019), tend to be weaker than their winter counterparts. This results in fewer summer anticyclones meeting the strength threshold to be classified as blocks and the resultant lower climatological blocking frequency.

4.2 Euro-Atlantic and Pacific Block Persistence Distribution

While Fig. 4 implicitly shows how many days in each season are blocked on average, the length of each individual block can vary greatly around its average length. Figure 4 also does not consider the spatial scale of blocking events. The distribution of sector block persistence for the ATL and PAC regions is shown in Fig. 5, along with the 25th, 50th and 75th percentiles. Results for winter and summer are discussed in detail here since these are the seasons where blocking has the potential to bring the most severe hazards. However, spring and autumn blocks can also be important for agriculture and harvests, and the histograms for these two seasons are shown in Sect. A1. Block events with a persistence of fewer than 5 days (despite the 5-day persistence criterion at grid-point level) represent a group of grid points within the sector that meet the sector block area

https://doi.org/10.5194/wcd-2022-59
Preprint. Discussion started: 28 November 2022

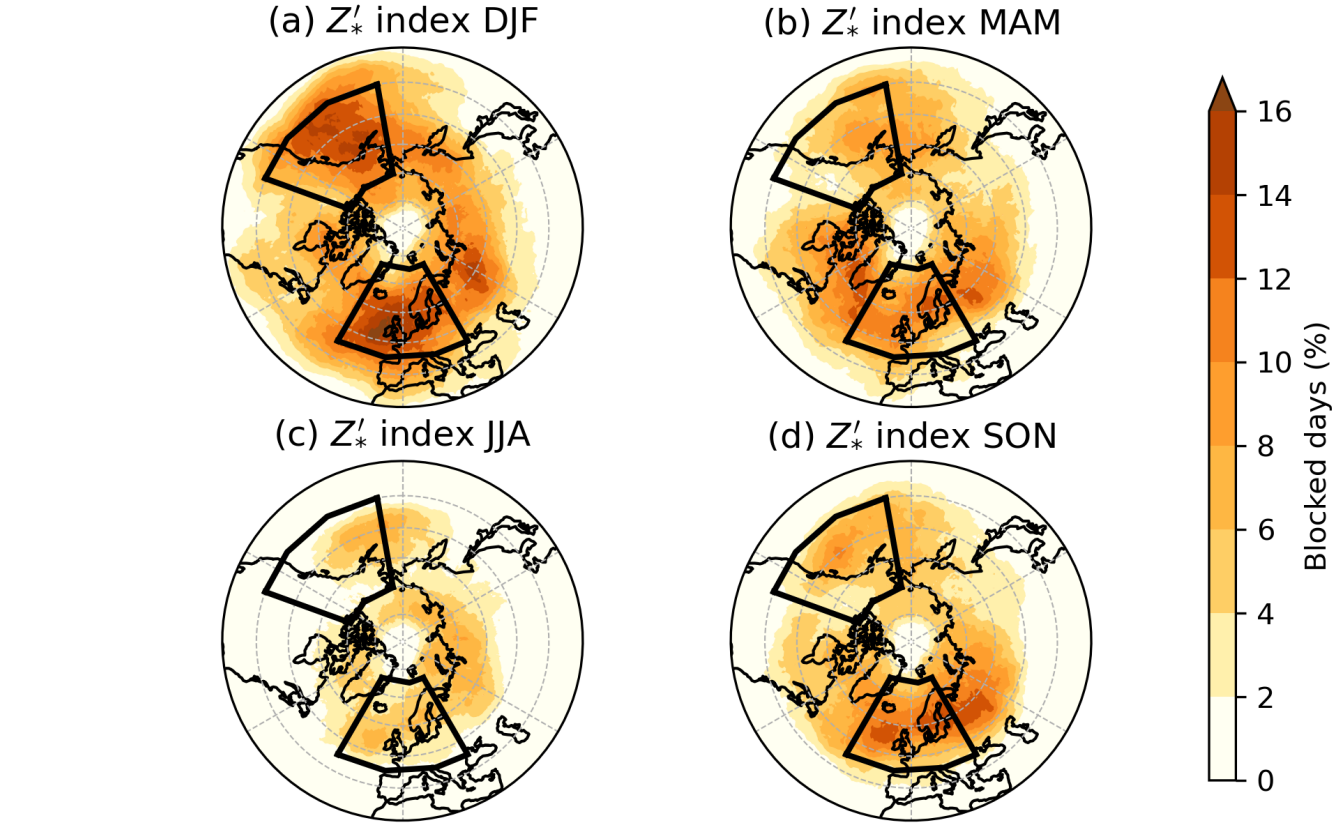

Figure 4. Blocked day frequency according to the Z'_* index, showing the percentage of days in a season that are blocked in (a) winter, DJF; (b) spring, MAM; (c) summer, JJA; and (d) autumn, SON. Black boxes indicate the ATL and PAC regions.

criterion for fewer than 5 days. These events are either small in size, or occur on the very edges of the domains. Only blocks with an onset in a particular season are included in the results for that same season.

The distributions are skewed towards shorter block persistences in all seasons in both domains (peaking at 6–7 days), though the tails of the distributions towards larger persistences are long. In this way, the shape of the persistence distribution in Fig. 5 of beyond 5 days is qualitatively similar to the distributions found in other studies that use different blocking indices (e.g., Wiedenmann et al., 2002; Diao et al., 2006; Drouard and Woollings, 2018; Detring et al., 2020). However, there is also a secondary peak in block length further towards longer persistences (around 15 days), particularly for DJF ATL blocks, which has not been found in previous studies.

https://doi.org/10.5194/wcd-2022-59
Preprint. Discussion started: 28 November 2022

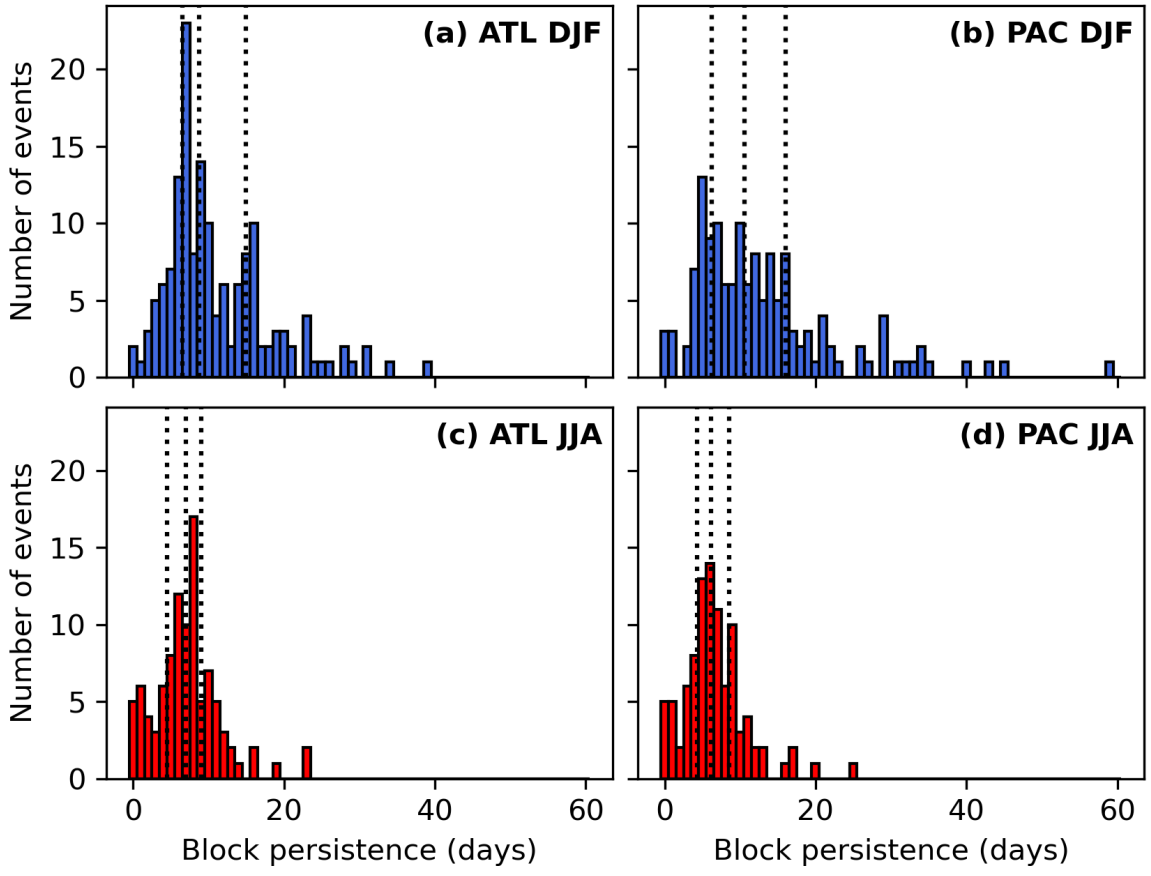

Figure 5. Histograms showing sector blocking event persistence frequency in winter (a, b) and summer (c, d) for the ATL (a, c) and PAC (b, d) sectors. The 25th, 50th, and 75th percentiles of block persistence in each panel are shown by the vertical dotted lines.

In the ATL region, the distribution of block persistence is remarkably similar for DJF, MAM, and SON (25th percentile of $\sim$ 6 days, median of $\sim$ 9 days, 75th percentile of 12–14 days). The longest blocks in this domain are found in DJF and SON, lasting 39.25 and 39.75 days respectively. In summer however, the distribution is different and the tail is not as long, with the quartiles being 4.5, 7, and 9 days respectively, and the longest summer ATL block is only 23 days long. Slightly more seasonal variation with block persistence is found in the PAC region, and with the exception of winter, PAC blocks are generally slightly shorter than in the ATL domain. Winter PAC blocks have the largest 50th and 75th percentiles (10.63, and 16 days), and the longest block by far occurs in the PAC region during winter (59 days). This extraordinarily persistent event resulted from two large-scale transient ridges which both stopped propagating in the PAC region. A long, 44-day block is also found in spring,

https://doi.org/10.5194/wcd-2022-59
Preprint. Discussion started: 28 November 2022

though the median block length at 8 days is smaller than for winter. As in the ATL region, summer PAC blocks are much shorter than at other times of the year (e.g. the 75th percentile is only 8.57 days). In both regions, MAM and SON blocks are distributed similarly to those in DJF (Sect. A1).

5 Relationship between Block Persistence AC Transient Eddies

5.1 Number of AC Eddies

The persistence, mean area, and number of associated transient AC eddy tracks of each blocking event for both regions in winter and summer are shown in Fig. 6. As with the histograms in Fig. 5, MAM and SON blocks behave similarly to DJF blocks in terms of AC eddy number, thus only winter and summer blocks are discussed here, with results from MAM and SON discussed in Sect. A2.

Longer blocks are generally larger, and this relationship is strongest in winter in the PAC (Table 1). Larger blocks would require more forcing from upstream to make them decay, so this result is not surprising. Additionally, more persistent blocks generally have more transient AC eddies contributing to them, and this is a combination of a larger number of these eddies either ending in or passing through the block. The correlation between block persistence and block area is comparable to the correlation between persistence and number of AC eddy interactions in DJF for both sectors (Table 1). The JJA correlations between persistence and number of AC eddies are weaker but still reasonably strong, suggesting that the number of AC eddy interactions with a block is less important in summer (this can also be observed in Fig. 6). The relationship between the area of a block and the number of AC eddies it interacts with is comfortably the smallest of the three quantities shown in Table 1, and is insignificant in the ATL region in JJA. For a given area, there is large variability in the number of AC eddies a block interacts with (Fig. 6).

Despite the general observation where more persistent blocks interact with more AC eddies, there is also substantial variability in the number of AC eddies for a block of given persistence, where between 2 and 6 eddies can be seen to be contributing the most persistent 25% of blocks (Fig. 6). The Pacific exhibits more interseasonal variability in terms of the average number of eddies per block than the Atlantic (Tables 2 and 3). The shortest 25% of winter ATL blocks have an average of 1.68 AC eddies contributing to them, and the longest 25% have three and a half times as many eddies (6.18) than the shortest 25%. However in the PAC sector, the longest 25% of blocks interact with five times as many AC eddies as the shortest 25% of blocks in this sector. The aforementioned 59-day DJF PAC block event interacted with eight upstream AC eddies. In summer, the longest 25% of blocks have three times as many AC eddies contributing to blocking than the shortest 25%, though due to the much shorter persistences in summer, the average number of AC eddies interacting with summer blocks is far smaller than in winter (Fig. 6, Tables 2 and 3).

https://doi.org/10.5194/wcd-2022-59
Preprint. Discussion started: 28 November 2022

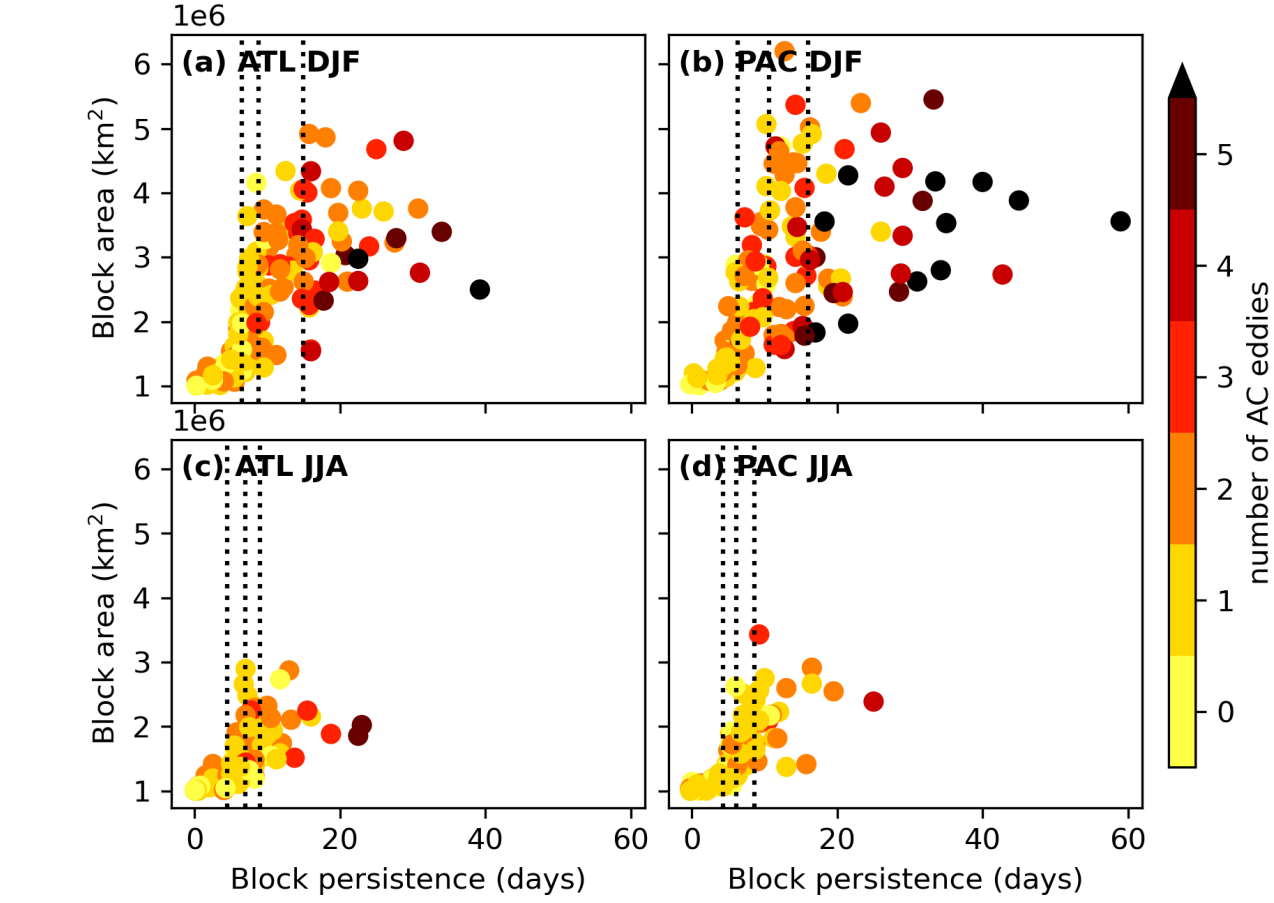

Figure 6. Number of anticyclonic transient eddies that contribute to blocking events in winter (a, b) and summer (c, d) for the ATL (a, c) and PAC (b, d) regions. Blocking events are characterised by their persistence and mean block area. 25th, 50th, and 75th percentiles of block persistence are shown by horizontal lines as in Fig. 5.

5.2 AC Eddy Strength and Speed for all Blocks

It is possible that the characteristics, in addition to the amount, of AC eddies interacting with a block can influence its persistence. First, the mean strength, as measured by the magnitude of Z'_* at the AC eddy centre, and zonal and meridional speeds of AC eddies are presented, for blocks of all persistences. A breakdown of these AC eddy quantities according to block persistence is discussed in Sect. 5.3.

Figure. 7 shows the strength, zonal speed and meridional speed of the AC eddies in the 7 days before and after entering either an ATL or a PAC block. The general behaviour of the eddies is similar in both the ATL and PAC regions. In the days

https://doi.org/10.5194/wcd-2022-59
Preprint. Discussion started: 28 November 2022

Table 1. Pearson's correlation coefficients between block characteristics. "Area" is the mean area of the block throughout its lifetime, "persist" is the block's persistence, and "eddies" is the number of anticyclonic eddies that pass through, or end in, the block. An italic number in parentheses indicates that the correlation coefficient is *not significant* at the 95% confidence level.

	ATL DJF	ATL JJA	PAC DJF	PAC JJA
Number of events	154	99	142	96
Area, persist	0.67	0.62	0.53	0.71
Area, eddies	0.32	*(0.24)*	0.29	0.31
Persist, eddies	0.63	0.53	0.77	0.46

Table 2. Basic AC eddy track statistics for ATL block events in DJF (JJA).

ATL Blocks	Quartile 1	Quartile 2	Quartile 3	Quartile 4
Block persistence (days)	$\leq$ 6.25 ($\leq$ 4.25)	6.50 – 8.75 (4.50 – 6.75)	9.00 – 14.75 (7.00 – 8.75)	$\geq$ 15.00 ($\geq$ 9.00)
Number of AC eddies	62 (26)	73 (43)	146 (57)	241 (81)
AC eddies per block (mean)	1.68 (1.08)	1.97 (1.72)	3.56 (2.38)	6.18 (3.12)

Table 3. As Table 2 but for the PAC region.

PAC Blocks	Quartile 1	Quartile 2	Quartile 3	Quartile 4
Block persistence (days)	$\leq$ 6.00 ($\leq$ 4.00)	6.25 – 10.50 (4.25 – 6.00)	10.75 – 15.75 (6.25 – 8.50)	$\geq$ 16.00 ($\geq$ 8.75)
Number of AC eddies	57 (19)	127 (42)	136 (39)	306 (61)
AC eddies per block (mean)	1.68 (0.83)	3.43 (1.68)	4.00 (1.63)	8.27 (2.54)

before the eddies enter a block, their strength (Fig. 7a, b) remains fairly constant in both DJF and JJA. AC eddies contributing to DJF ATL blocking are stronger than their PAC counterparts before entering the block. JJA eddies are of a similar strength in both domains, but weaker than those in DJF. In the ATL domain, AC eddies in both DJF and JJA strengthen by around 50 m in the first two days after they entering a block (time = 0 line in Fig. 7). In the PAC region, the intensification is stronger for DJF eddies (nearly 100 m) and begins at around day -3. This is potentially because the PAC region is slightly to the east of the North Pacific climatological blocking maximum (Fig. 4), meaning the AC eddies intensify upon entering the block while it is outside the domain. However, further intensification does occur once the eddies are inside a block in the PAC domain between days 0 and +1. After this, in both regions, there is a steady decay of the eddy strength (though they are still as intense or stronger than they were before blocking). However, the strength of the block can be maintained by the absorption of additional AC eddies later in its lifetime (not shown), if it persists for long enough.

The AC eddy zonal speed (Fig. 7c, d) is also fairly constant in the days before the eddy enters a block. Winter eddies move eastwards faster than those in summer, and the difference between seasons is largest in PAC. Upon entering the block, the eddies rapidly decelerate such that their zonal speed halves compared to days -7 to 0. Unlike with eddy strength, the zonal speed of the eddies remains constant through to day +7 and beyond.

https://doi.org/10.5194/wcd-2022-59
Preprint. Discussion started: 28 November 2022

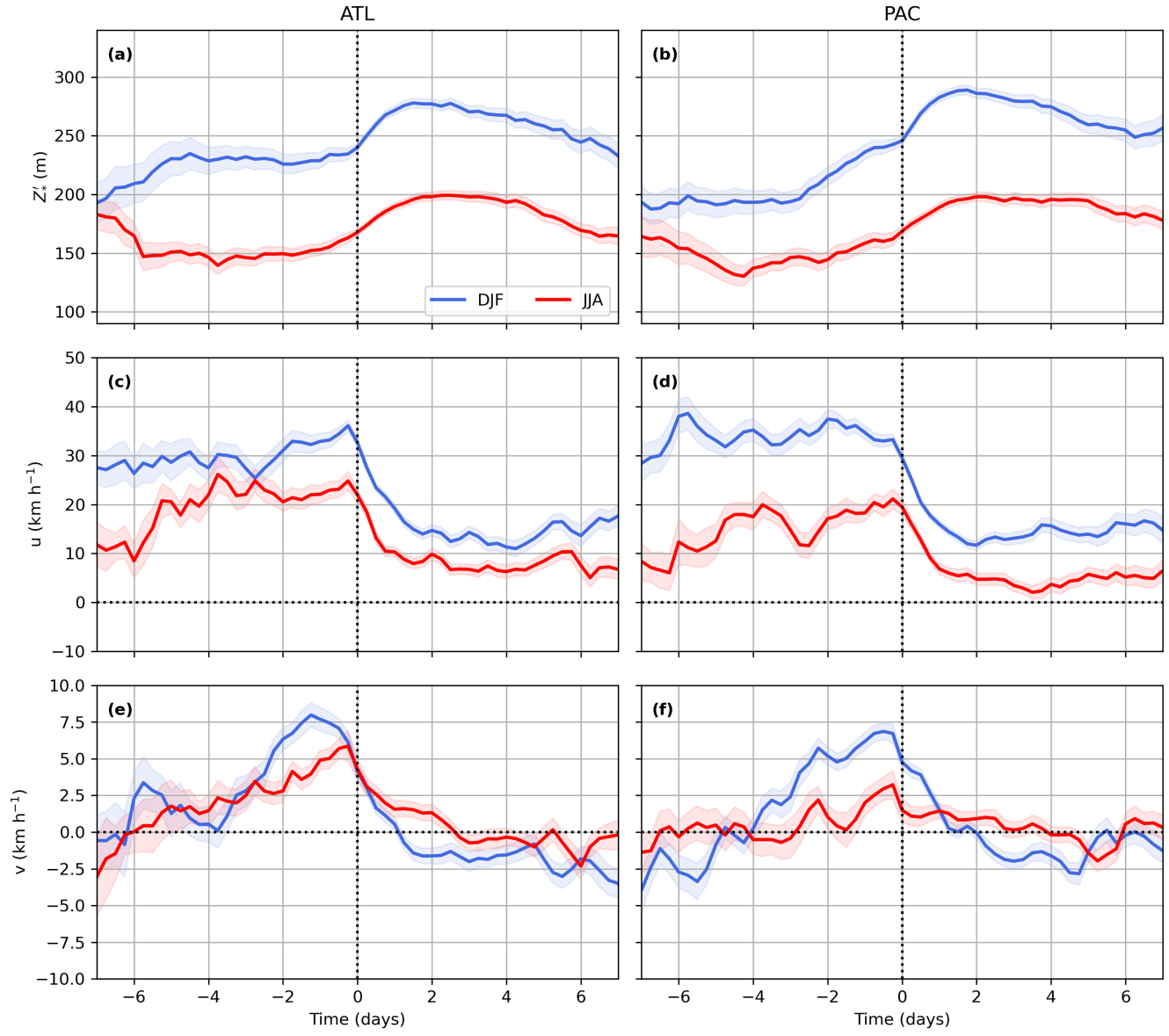

Figure 7. Characteristics of transient AC eddies that contribute to ATL blocks (a, c, e) and PAC blocks (b, d, f) during winter (blue), and summer (red). Strength of the eddy in terms of its maximum Z'_* (a, b), zonal velocity u (c, d), and meridional velocity v (e, f) are shown. Negative times indicate the period before the eddy enters a block in the domain, and positive times indicate times after entering a block. Solid lines show the mean characteristics, with shading signifying the standard error of each measure at each time step.

The evolution of the meridional speed of the AC eddies that contribute to blocking in both domains is more complex (Fig. 7e, f). In the seven days before entering a block, AC eddies gradually accelerate northwards in both domains during winter,

https://doi.org/10.5194/wcd-2022-59
Preprint. Discussion started: 28 November 2022

and in summer in the ATL, though their meridional speeds are around four times smaller than their zonal speeds (Fig. 7c, d). These eddies then rapidly decelerate meridionally once inside a block too, reaching weak southward speeds. The rapid deceleration of the eddies, both zonally and meridionally, is typical of blocking dynamics, since blocking systems are quasi-stationary. Meridional speed for PAC summer blocking AC eddies is fairly constant before and during blocking. This northward acceleration is potentially indicative of two things. Firstly, it signifies a building of a ridge through the northward advection of higher geopotential heights, which is a characteristic of blocking. However, it could also be the result of eddies being attracted by the block via the SAM, though a more detailed analysis on the vortex-vortex interactions between the block and the eddies would be required to verify this, which is beyond the scope of this study.

In MAM and SON (Sect. A3), AC eddies behave in largely the same way as outlined here, with intermediate speeds and strengths between those in DJF and JJA.

5.3 AC Eddy Strength and Speed for Blocks of Different Persistences

A similar analysis to that presented in Fig. 7 can be performed for AC eddies that interact with blocks with various persistences, to determine whether there is a relationship between the strength or speed of the eddies and the persistence of the blocks they contribute to. Figures 8 and 9 show the strength and speed of the AC eddies that interact with blocks of different persistences, determined by the quartile of block persistence, in DJF and JJA respectively. Analysis will be focused on the week before and after the AC eddies enter a block. The mean characteristics are shown by the lines, and standard error by the shading. If there is no overlap of the standard errors between AC eddy characteristics of different block persistences, then the results are said to be statistically significant.

The longest 50% of DJF ATL blocks interact with slightly stronger AC eddies than the least persistent 50% of blocks (Fig. 8a), with the mean eddy strength for the upper two quartiles being about 40 m stronger at the time that the eddies enter the block. However, AC eddies contributing to blocks with persistences in the fourth quartile in this domain and season are not stronger than those with persistences in the third quartile (likewise for the first and second quartile). In the PAC domain in winter (Fig. 8b), only AC eddies contributing to the most persistent 25% of blocks are significantly stronger than other AC eddies, with no statistically significant difference between AC eddy strength at time = 0 for AC eddies interacting with blocks of any other length. More persistent PAC blocks also result from the absorption of stronger AC eddies in MAM (Sect. A4). In both domains during summer, longer blocks are not the result of interacting with stronger AC eddies, since the standard errors between each quartile is overlapping with another (Fig. 9a-b). Likewise, there is no suggestion from Fig 8c-f that block persistence depends on the speed of the incoming AC eddies either.

It may appear from Figs. 8 and 9 that AC eddies that interact with the least persistent blocks become weaker and fast-moving again from day +4 onwards. To some extent, the same is true at times over +7 days for AC eddies that contribute to more persistent blocks (not shown). While it is true that such AC eddies do weaken and speed up at these times, the block is no longer present at these time steps, so these eddies are no longer contributing with blocks. However, there appears to be a significant result in the PAC domain for DJF in that the least persistent blocks are associated with the strongest AC eddies at around day -4 (Fig. 8b), where the mean eddy strength is considerably higher than for eddies contributing to longer blocks.

https://doi.org/10.5194/wcd-2022-59
Preprint. Discussion started: 28 November 2022

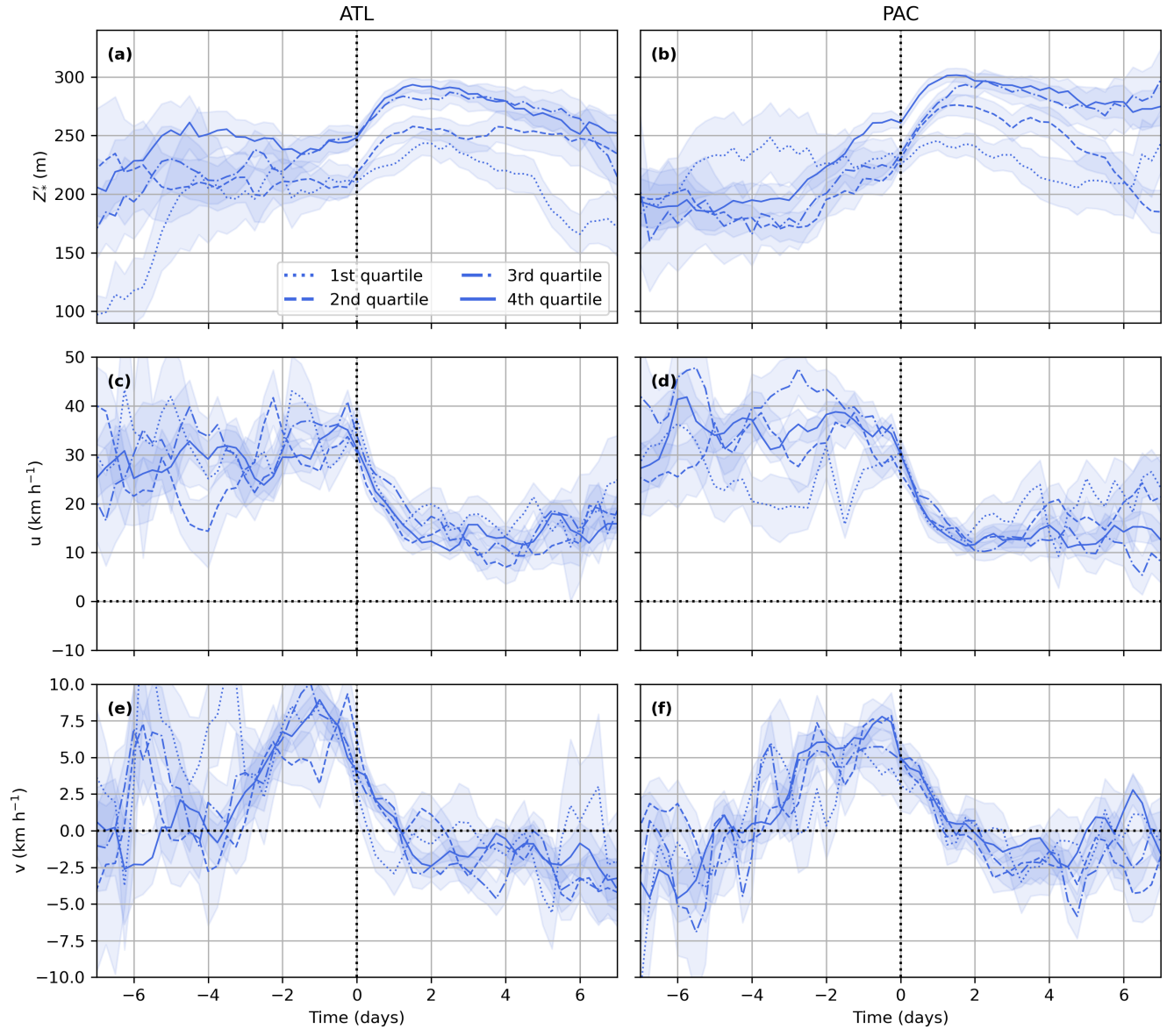

Figure 8. As in Fig. 7, but showing the characteristics of AC eddies that contribute to blocks of different persistences, for DJF only. Block persistence is determined by the percentiles shown in Fig. 5. The mean characteristics of the AC eddies contributing to blocks with a persistence in the first quartile (least persistent) are shown in dotted lines, second quartile in dashed lines, third quartile in dash-dotted lines, and fourth quartile (most persistent) in a solid line.

In all domains at all times of year, AC eddies that contribute to the shortest 25% of blocks do not markedly intensify upon entering a block like those entering longer blocks do, underlying the more transient nature of these shorter-lived block events.

https://doi.org/10.5194/wcd-2022-59
Preprint. Discussion started: 28 November 2022

It is therefore possible that the lack of intensification of AC eddies upon entering a block could be a signal that the block will not persist.

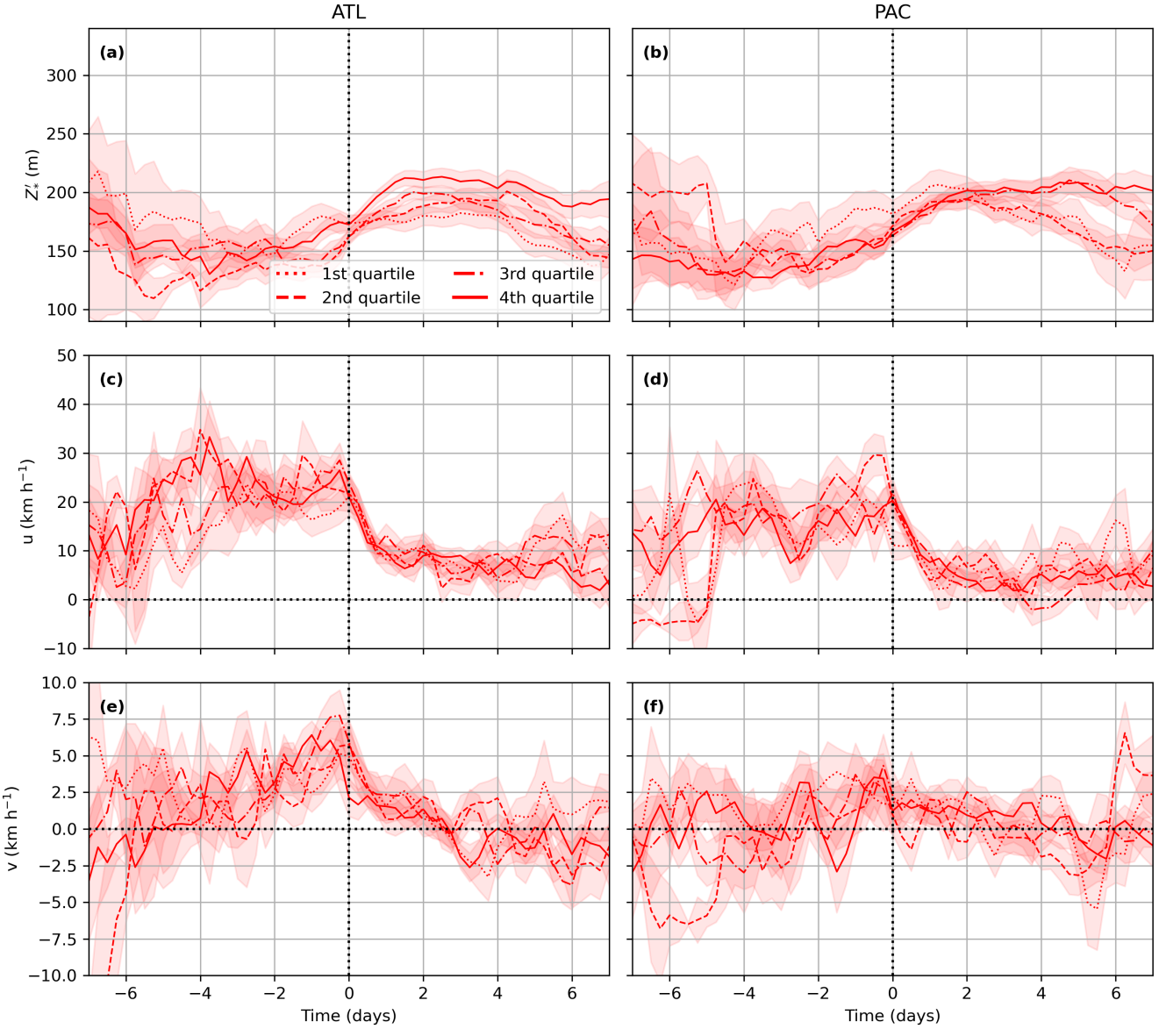

Figure 9. As in Fig. 8, but for JJA only.

https://doi.org/10.5194/wcd-2022-59
Preprint. Discussion started: 28 November 2022

6 Conclusions

This study has used objective feature-tracking of synoptic-scale AC eddies that help to maintain atmospheric blocking events. The climatological relationship between transient AC eddy number, intensity, and block persistence in the North Pacific (PAC) and Euro-Atlantic (ATL) regions are analysed. It is found that in both sectors, more persistent blocks are associated with more transient AC eddies, and this relationship is weaker in summer compared to other times of the year. The PAC region exhibits a larger variability in the number of eddy interactions for blocks of different lengths than the ATL region, though both regions show that the most persistent blocks interact with the most AC eddies. These results suggest that blocks can be maintained through repeated absorption of AC eddies, potentially supporting the SAM theory (Yamazaki and Itoh, 2013a). In general, the number of AC eddies a block interacts with is important for determining its persistence. However, not all persistent blocks are the result of a large number of AC eddy interactions, which indicates that other dynamical processes are also important for block maintenance in these cases.

In addition, there is a less clear relationship between block persistence and the strength of the AC eddies that it absorbs. In winter, the longest 50% of ATL blocks and 25% of PAC blocks absorb slightly stronger AC eddies than shorter blocks. Aside from this, there is no significant difference between the strength of AC eddies absorbed for blocks of varying persistences. Block persistence is thus largely independent on the strength (and speed) of the AC eddies it interacts with. Analysis of AC transient eddies associated with blocks of all lengths, however, leads us to conclude that winter eddies are stronger and faster than their summer counterparts. AC eddies intensify and accelerate northwards towards the block just before entering, which could potentially signal an attraction via the Selective Absorption Mechanism (SAM, Yamazaki and Itoh (2013a)). Nonetheless, though more evidence is required to ascertain whether this is actually observed. However, AC eddies that enter the least persistent 25% of blocks do not undergo this intensification once inside the block, and this behaviour could be used as a potential indicator for how long a block may persist for. All AC eddies rapidly decelerate once inside a block, consistent with the slow-moving nature of block events.

This study only considers dry dynamical processes, namely multi-scale interaction between the large-scale blocks and smaller-scale AC eddies. While the results presented here suggest there is a strong, significant relationship between block persistence and the amount of AC eddies a block interacts with, this process is certainly not the only dynamical process occurring during the maintenance phase of a block. The most important missing piece of this study is the extent to which moist dynamics, for example diabatically-heated outflow from warm conveyer belts (e.g. Pfahl et al., 2015; Steinfeld and Pfahl, 2019), also affect block persistence. We hypothesise that in persistent blocks with very few AC eddy interactions, other maintenance processes such as diabatically-generated negative PV anomalies are instead dominant. Similarly, in short blocks with many AC eddy interactions, there may be other processes (e.g. diabatic cooling) that causes the block to decay quickly despite the continued AC eddy forcing. Further work is required to compare these dynamical differences between blocks with many contributing AC eddies to those with few AC eddy contributions.

https://doi.org/10.5194/wcd-2022-59
Preprint. Discussion started: 28 November 2022

Weather and Climate Dynamics Discussions
Open Access
EGU

Code and data availability. The code used to obtain the results in this work are available from the authors upon request. The underlying data used for the analysis can be obtained from the ECMWF ERA5 reanalysis website: (https://www.ecmwf.int/en/forecasts/datasets/reanalysisdatasets/era5, European Centre for Medium-Range Weather Forecasts, 2022). TRACK is available for download from https://gitlab.act.reading.ac.uk/track/track.

Appendix A

A1 Block Persistence Distribution for MAM and SON

Histograms showing the block persistence distribution for MAM and SON in both the ATL and PAC regions is shown in Fig. A1. The distributions are broadly similar to those found in DJF for the respective regions, with similar 25th, 50th, and 75th percentile values.

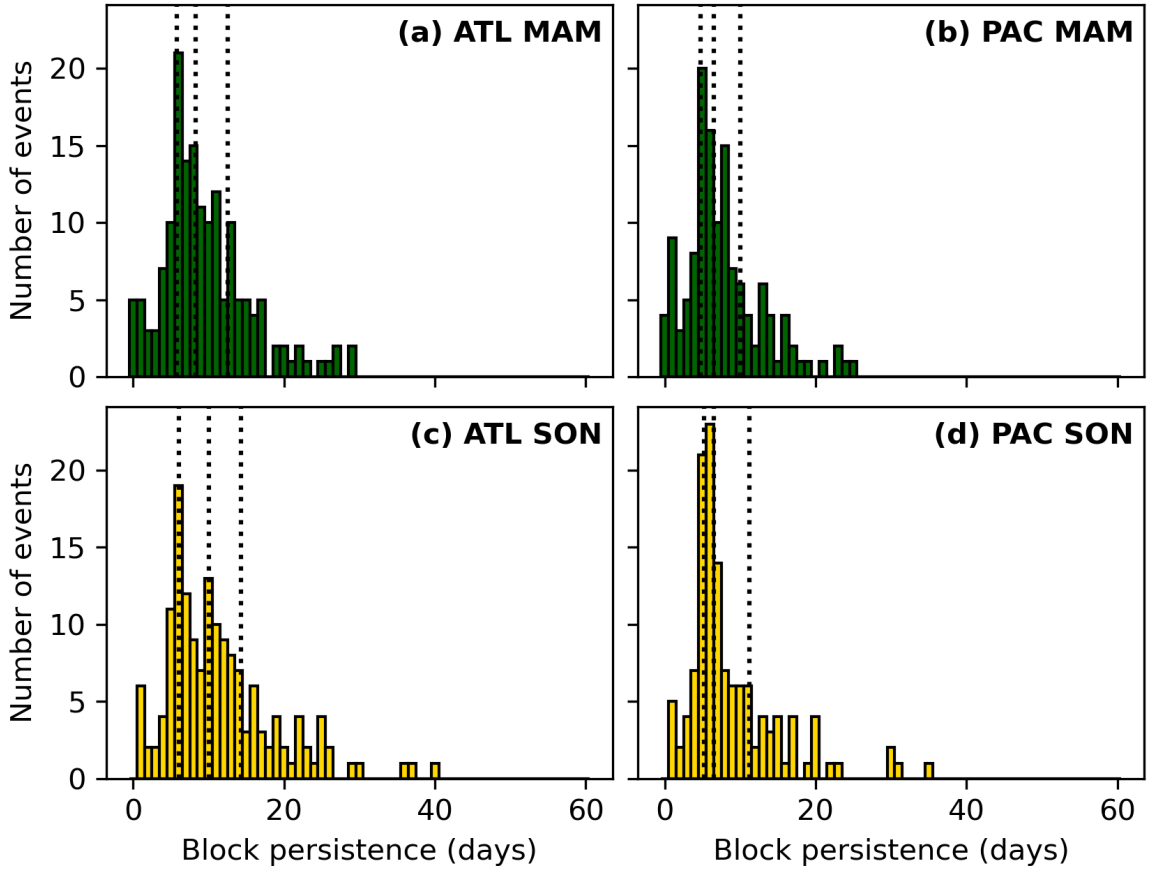

Figure A1. As in Fig. 5, but for MAM (a, c) and SON (b, d).

https://doi.org/10.5194/wcd-2022-59
Preprint. Discussion started: 28 November 2022

A2 Number of AC Eddies Contributing to MAM and SON Blocks

The relationship between block area, persistence, and number of contributing AC eddies for MAM and SON for both the ATL and PAC domains is shown in Fig. A2. In both domains in both seasons here, the general patterns between the three variables is the same as those found in DJF. Pearson correlation coefficients are as high they are in DJF for these seasons between block persistence and the number of AC eddies (0.59–0.71), block persistence and area (0.62–0.73), and number of AC eddies and block area (0.32–0.45).

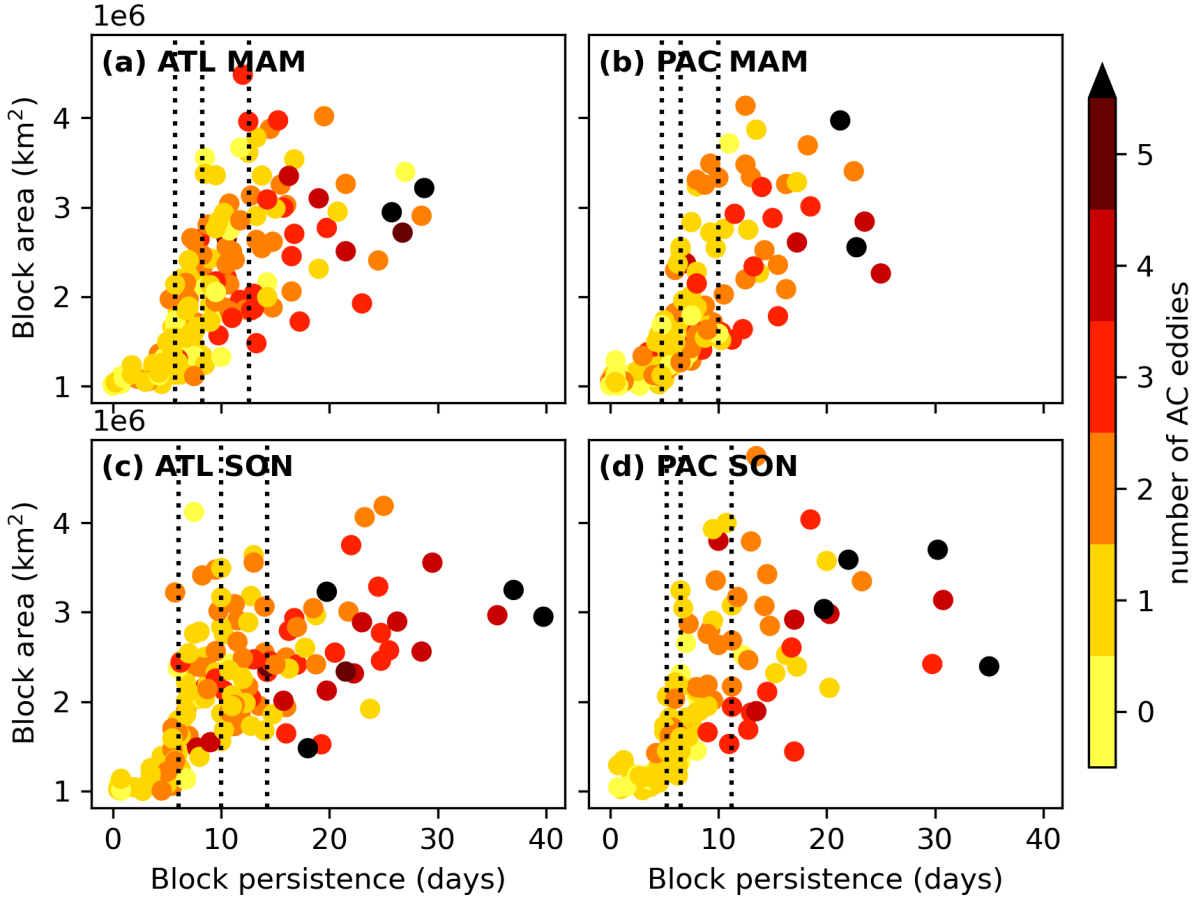

Figure A2. As Fig. 6, but for MAM (a, c) and JJA (b, d).

https://doi.org/10.5194/wcd-2022-59
Preprint. Discussion started: 28 November 2022

Weather and Climate Dynamics Discussions
Open Access
EGU

A3 AC Eddy Strength and Speed for all Blocks in MAM and SON

The mean and standard error of the AC eddy intensity and speed before and during/after blocking for MAM and SON is shown in Fig. A3. The eddies exhibit the same qualitative characteristics as those in DJF and JJA, with intermediate values. Both speed and intensity for MAM and SON are very similar to each other too.

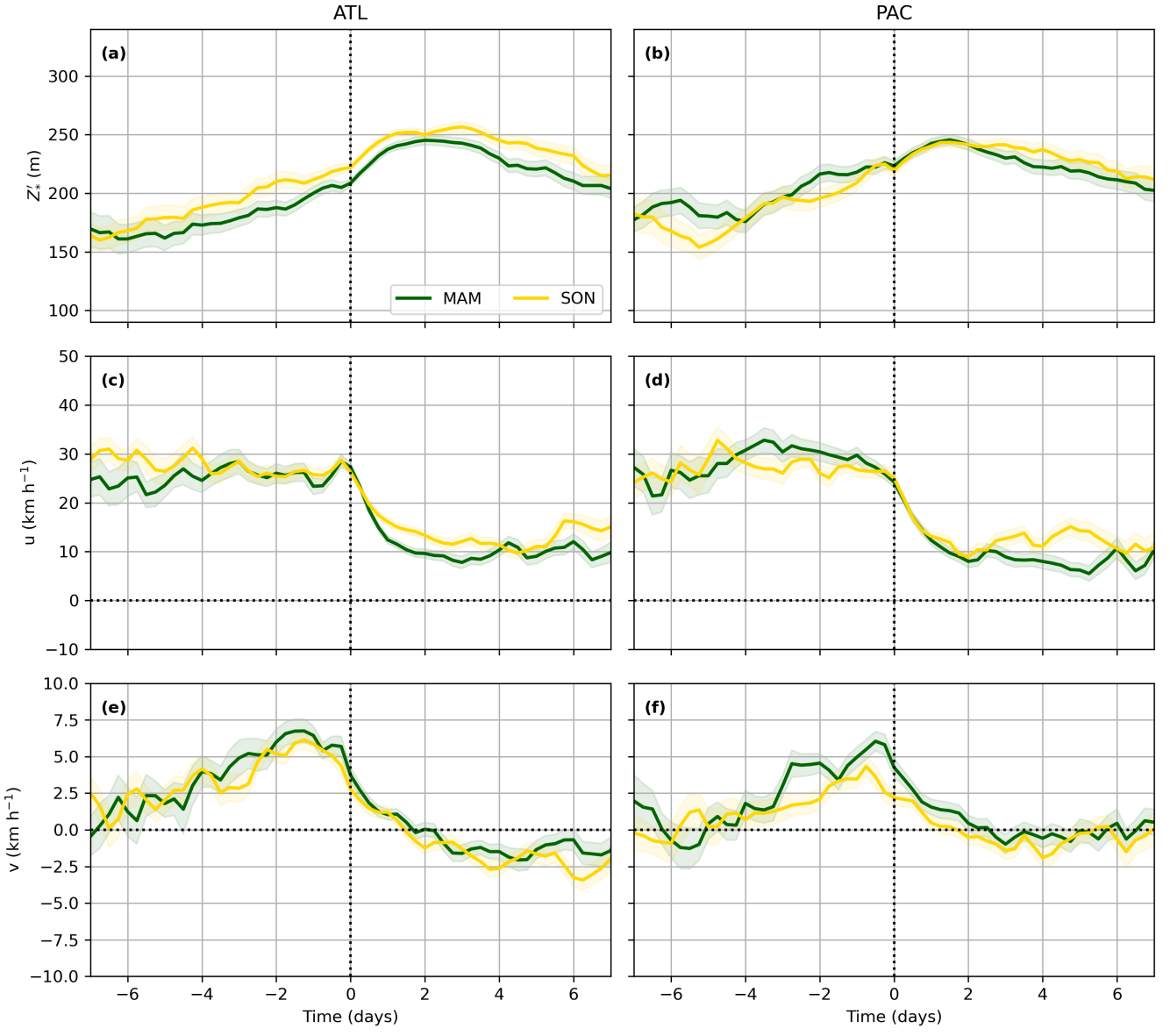

Figure A3. As in Fig. 7, but for MAM (green) and SON (yellow).

https://doi.org/10.5194/wcd-2022-59
Preprint. Discussion started: 28 November 2022

A4 AC Eddy Strength and Speed for Blocks of Different Lengths in MAM and SON

AC eddy speed and strength for blocks of different lengths for MAM and SON is shown in Figs. A4 and A5. Generally, like in JJA and DJF, the strength and speed of the eddy is independent of the persistence of the block it contributes to. However, MAM PAC eddies appear to also show some variation in their strength according to how long the block is, but the standard errors are large and sometimes overlapping.

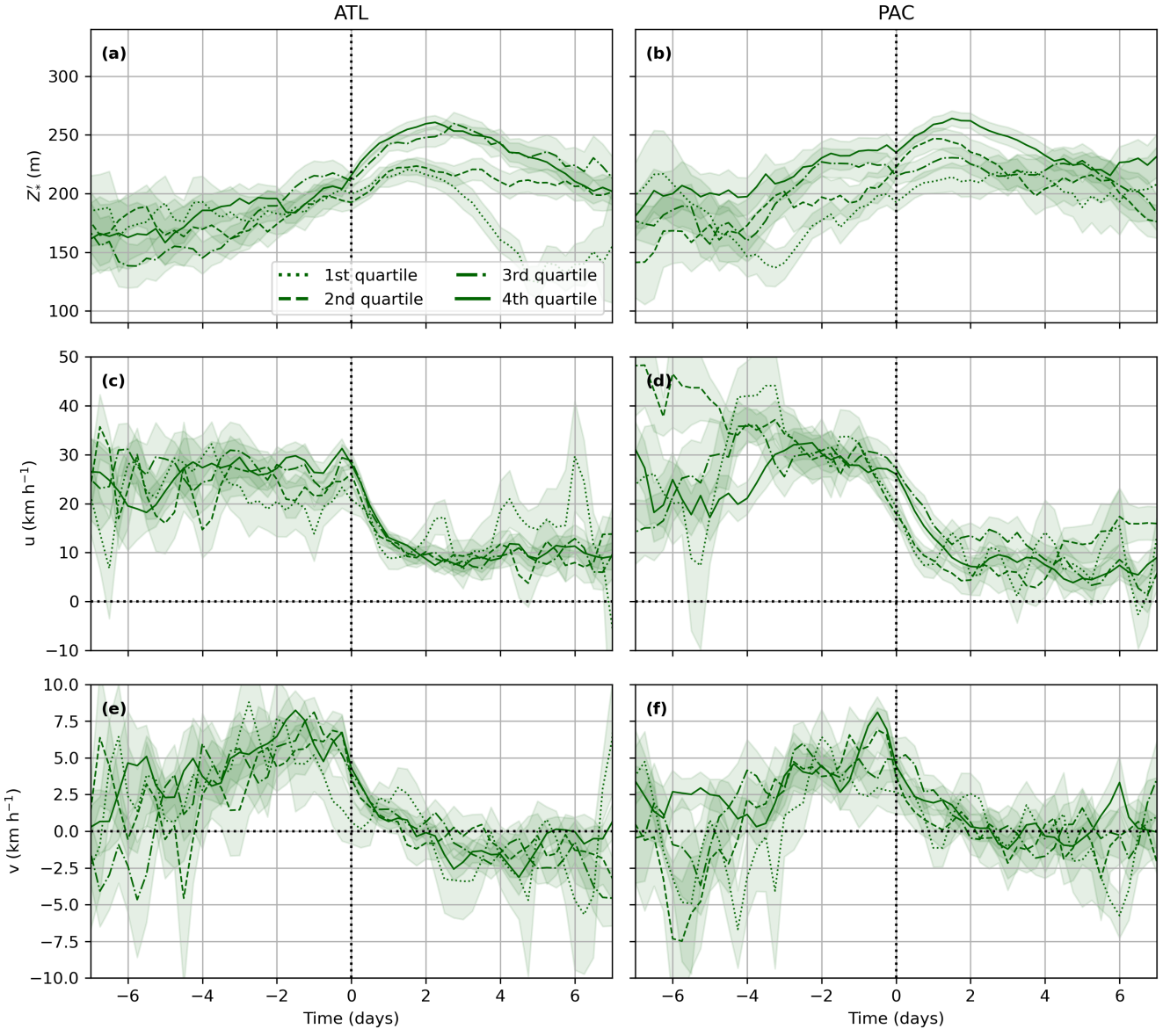

Figure A4. As in Fig. 8, but for MAM.

https://doi.org/10.5194/wcd-2022-59
Preprint. Discussion started: 28 November 2022

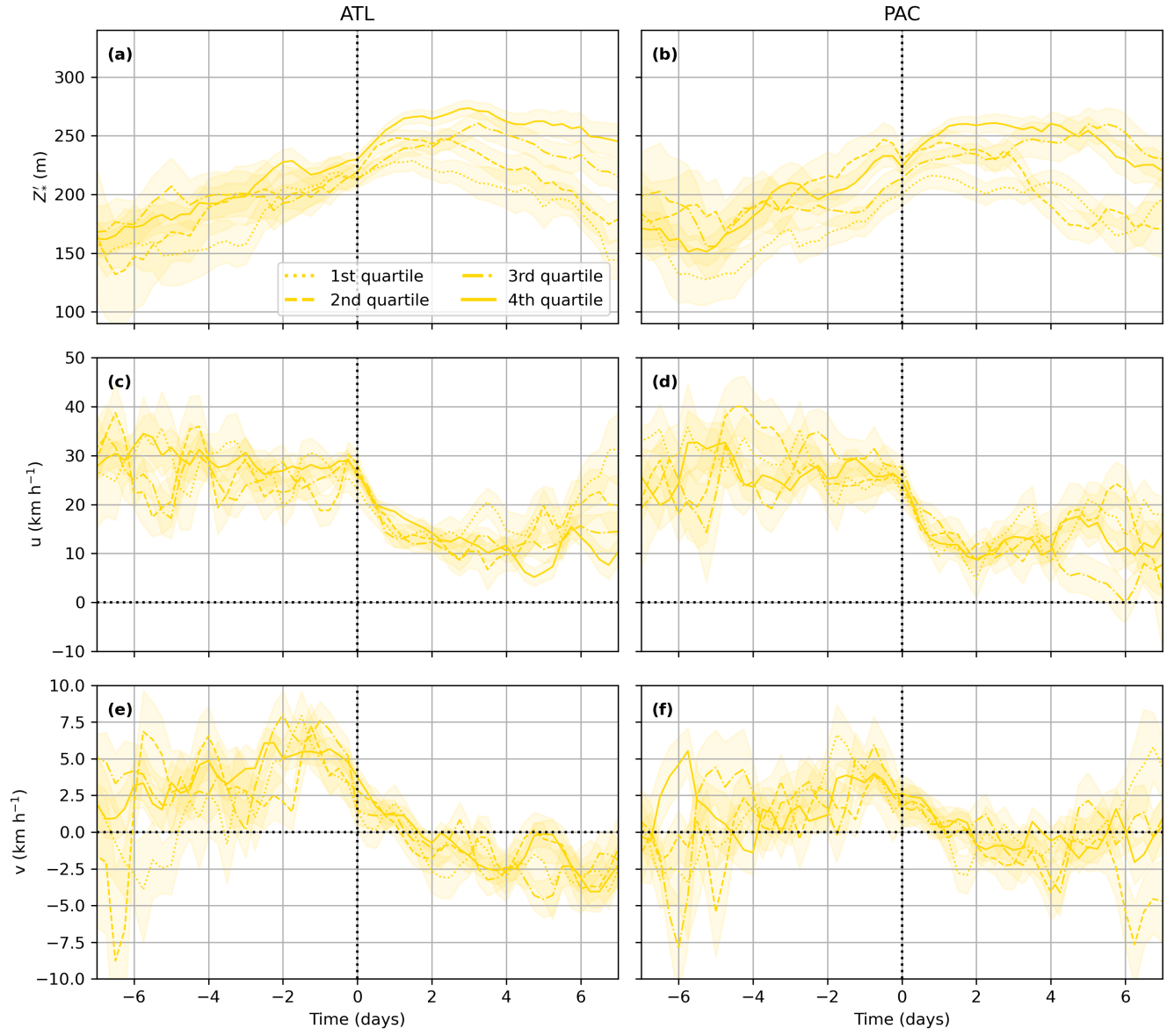

Figure A5. As in Fig. 8, but for SON.

Author contributions. CCS developed the blocking index, sector blocking definition, and the analysis of the results. OM-A, KIH, RKHS and DA secured PhD project funding for this work. KIH provided access to, and guidance with using TRACK. The manuscript was written by CCS, with support from OM-A, KIH, RKHS, and DA.

https://doi.org/10.5194/wcd-2022-59
Preprint. Discussion started: 28 November 2022

Competing interests. The authors declare that they have no conflict of interest.

Acknowledgements. CCS is funded by the Natural Environment Research Council (NERC) via the SCENARIO Doctoral Training Partnership (Grant NE/S0077261/1) with additional CASE funding from the UK Met Office. OM-A, KIH and RKHS are supported by the U.K. National Centre for Atmospheric Science (NCAS) at the University of Reading (R8/H12/83/007). DA is supported by the Joint BEIS/Defra Met Office Hadley Centre Climate Programme (GA01101).

https://doi.org/10.5194/wcd-2022-59
Preprint. Discussion started: 28 November 2022

References

Altenhoff, A. M., Martius, O., Croci-Maspoli, M., Schwierz, C., and Davies, H. C.: Linkage of atmospheric blocks and synoptic-scale Rossby waves: A climatological analysis, Tellus A: Dynamic Meteorology and Oceanography, 60, 1053–1063, 2008.

Austin, J.: The blocking of middle latitude westerly winds by planetary waves, Quarterly Journal of the Royal Meteorological Society, 106, 327–350, 1980.

Barnes, E. A., Slingo, J., and Woollings, T.: A methodology for the comparison of blocking climatologies across indices, models and climate scenarios, Climate dynamics, 38, 2467–2481, 2012.

Barriopedro, D., García-Herrera, R., and Trigo, R. M.: Application of blocking diagnosis methods to general circulation models. Part I: A novel detection scheme, Climate dynamics, 35, 1373–1391, 2010.

Büeler, D., Ferranti, L., Magnusson, L., Quinting, J. F., and Grams, C. M.: Year-round sub-seasonal forecast skill for Atlantic–European weather regimes, Quarterly Journal of the Royal Meteorological Society, 147, 4283–4309, 2021.

Catto, J. L., Shaffrey, L. C., and Hodges, K. I.: Northern Hemisphere extratropical cyclones in a warming climate in the HiGEM high-resolution climate model, Journal of Climate, 24, 5336–5352, 2011.

Charney, J., Shukla, J., and Mo, K.: Comparison of a barotropic blocking theory with observation, Journal of Atmospheric Sciences, 38, 762–779, 1981.

Chen, L., Tan, B., Kvamstø, N. G., and Johannessen, O. M.: Wintertime cyclone/anticyclone activity over China and its relation to upper tropospheric jets, Tellus A: Dynamic Meteorology and Oceanography, 66, 21 889, 2014.

Colucci, S. J.: Explosive cyclogenesis and large-scale circulation changes: Implications for atmospheric blocking, Journal of Atmospheric Sciences, 42, 2701–2717, 1985.

Detring, C., Müller, A., Schielicke, L., Névir, P., and Rust, H. W.: Atmospheric blocking types: Frequencies and transitions, Weather and Climate Dynamics Discussions, 2020, 1–33, 2020.

Diao, Y., Li, J., and Luo, D.: A new blocking index and its application: Blocking action in the Northern Hemisphere, Journal of Climate, 19, 4819–4839, 2006.

Dole, R. M. and Gordon, N. D.: Persistent anomalies of the extratropical Northern Hemisphere wintertime circulation: Geographical distribution and regional persistence characteristics, Monthly Weather Review, 111, 1567–1586, 1983.

Drouard, M. and Woollings, T.: Contrasting mechanisms of summer blocking over western Eurasia, Geophysical Research Letters, 45, 12–040, 2018.

Drouard, M., Woollings, T., Sexton, D. M., and McSweeney, C. F.: Dynamical differences between short and long blocks in the Northern Hemisphere, Journal of Geophysical Research: Atmospheres, 126, e2020JD034 082, 2021.

Grams, C. M., Beerli, R., Pfenninger, S., Staffell, I., and Wernli, H.: Balancing Europe's wind-power output through spatial deployment informed by weather regimes, Nature climate change, 7, 557–562, 2017.

Hersbach, H., Bell, B., Berrisford, P., Hirahara, S., Horányi, A., Muñoz-Sabater, J., Nicolas, J., Peubey, C., Radu, R., Schepers, D., et al.: The ERA5 global reanalysis, Quarterly Journal of the Royal Meteorological Society, 146, 1999–2049, 2020.

Hodges, K.: A general method for tracking analysis and its application to meteorological data, Monthly Weather Review, 122, 2573–2586, 1994.

Hodges, K.: Feature tracking on the unit sphere, Monthly Weather Review, 123, 3458–3465, 1995.

Hodges, K.: Adaptive constraints for feature tracking, Monthly Weather Review, 127, 1362–1373, 1999.

https://doi.org/10.5194/wcd-2022-59
Preprint. Discussion started: 28 November 2022

Hodges, K. I., Lee, R. W., and Bengtsson, L.: A comparison of extratropical cyclones in recent reanalyses ERA-Interim, NASA MERRA, NCEP CFSR, and JRA-25, Journal of Climate, 24, 4888–4906, 2011.

Hoskins, B. and Hodges, K.: The annual cycle of Northern Hemisphere storm tracks. Part I: Seasons, Journal of Climate, 32, 1743–1760, 2019.

Ioannidou, L. and Yau, M.: A climatology of the Northern Hemisphere winter anticyclones, Journal of Geophysical Research: Atmospheres, 113, 2008.

Kautz, L.-A., Martius, O., Pfahl, S., Pinto, J. G., Ramos, A. M., Sousa, P. M., and Woollings, T.: Atmospheric blocking and weather extremes over the Euro-Atlantic sector–a review, Weather and Climate Dynamics, 3, 305–336, 2022.

Legras, B. and Ghil, M.: Persistent anomalies, blocking and variations in atmospheric predictability, Journal of Atmospheric Sciences, 42, 433–471, 1985.

Lejenäs, H. and Økland, H.: Characteristics of Northern Hemisphere blocking as determined from a long time series of observational data, Tellus A, 35, 350–362, 1983.

Lenggenhager, S. and Martius, O.: Quantifying the link between heavy precipitation and Northern Hemisphere blocking—A Lagrangian analysis, Atmospheric science letters, 21, e999, 2020.

Liu, P., Zhu, Y., Zhang, Q., Gottschalck, J., Zhang, M., Melhauser, C., Li, W., Guan, H., Zhou, X., Hou, D., et al.: Climatology of tracked persistent maxima of 500-hPa geopotential height, Climate Dynamics, 51, 701–717, 2018.

Lupo, A. R.: Atmospheric blocking events: a review, Annals of the New York Academy of Sciences, 1504, 5–24, 2021.

Masato, G., Hoskins, B., and Woollings, T. J.: Wave-breaking characteristics of midlatitude blocking, Quarterly Journal of the Royal Meteorological Society, 138, 1285–1296, 2012.

Miller, D. E. and Wang, Z.: Northern Hemisphere Winter Blocking: Differing Onset Mechanisms across Regions, Journal of the Atmospheric Sciences, 2022.

Mullen, S. L.: Transient eddy forcing of blocking flows, Journal of Atmospheric Sciences, 44, 3–22, 1987.

Nakamura, N. and Huang, C. S.: Atmospheric blocking as a traffic jam in the jet stream, Science, 361, 42–47, 2018.

Pelly, J. L. and Hoskins, B. J.: A new perspective on blocking, Journal of the atmospheric sciences, 60, 743–755, 2003.

Pepler, A., Dowdy, A., and Hope, P.: A global climatology of surface anticyclones, their variability, associated drivers and long-term trends, Climate Dynamics, 52, 5397–5412, 2019.

Pfahl, S., Schwierz, C., Croci-Maspoli, M., Grams, C. M., and Wernli, H.: Importance of latent heat release in ascending air streams for atmospheric blocking, Nature Geoscience, 8, 610–614, 2015.

Priestley, M. D., Ackerley, D., Catto, J. L., Hodges, K. I., McDonald, R. E., and Lee, R. W.: An overview of the extratropical storm tracks in CMIP6 historical simulations, Journal of Climate, 33, 6315–6343, 2020.

Rex, D. F.: Blocking action in the middle troposphere and its effect upon regional climate, Tellus, 2, 275–301, 1950.

Sainsbury, E. M., Schiemann, R. K., Hodges, K. I., Shaffrey, L. C., Baker, A. J., and Bhatia, K. T.: How important are post-tropical cyclones for European windstorm risk?, Geophysical Research Letters, 47, e2020GL089 853, 2020.

Scherrer, S. C., Croci-Maspoli, M., Schwierz, C., and Appenzeller, C.: Two-dimensional indices of atmospheric blocking and their statistical relationship with winter climate patterns in the Euro-Atlantic region, International Journal of Climatology: A Journal of the Royal Meteorological Society, 26, 233–249, 2006.

https://doi.org/10.5194/wcd-2022-59
Preprint. Discussion started: 28 November 2022

Schiemann, R., Demory, M.-E., Shaffrey, L. C., Strachan, J., Vidale, P. L., Mizielinski, M. S., Roberts, M. J., Matsueda, M., Wehner, M. F., and Jung, T.: The resolution sensitivity of Northern Hemisphere blocking in four 25-km atmospheric global circulation models, Journal of Climate, 30, 337–358, 2017.

Schiemann, R., Athanasiadis, P., Barriopedro, D., Doblas-Reyes, F., Lohmann, K., Roberts, M. J., Sein, D. V., Roberts, C. D., Terray, L., and Vidale, P. L.: Northern Hemisphere blocking simulation in current climate models: evaluating progress from the Climate Model Intercomparison Project Phase 5 to 6 and sensitivity to resolution, Weather and Climate Dynamics, 1, 277–292, 2020.

Schwierz, C., Croci-Maspoli, M., and Davies, H.: Perspicacious indicators of atmospheric blocking, Geophysical research letters, 31, 2004.

Shukla, J. and Mo, K.: Seasonal and geographical variation of blocking, Monthly Weather Review, 111, 388–402, 1983.

Shutts, G.: The propagation of eddies in diffluent jetstreams: Eddy vorticity forcing of 'blocking' flow fields, Quarterly Journal of the Royal Meteorological Society, 109, 737–761, 1983.

Sousa, P. M., Barriopedro, D., García-Herrera, R., Woollings, T., and Trigo, R. M.: A new combined detection algorithm for blocking and subtropical ridges, Journal of Climate, 34, 7735–7758, 2021.

Steinfeld, D. and Pfahl, S.: The role of latent heating in atmospheric blocking dynamics: a global climatology, Climate Dynamics, 53, 6159–6180, 2019.

Thomas, C., Voulgarakis, A., Lim, G., Haigh, J., and Nowack, P.: An unsupervised learning approach to identifying blocking events: the case of European summer, Weather and Climate Dynamics, 2, 581–608, 2021.

Tibaldi, S. and Molteni, F.: On the operational predictability of blocking, Tellus A, 42, 343–365, 1990.

Tyrlis, E. and Hoskins, B.: Aspects of a Northern Hemisphere atmospheric blocking climatology, Journal of the atmospheric sciences, 65, 1638–1652, 2008.

Vautard, R.: Multiple weather regimes over the North Atlantic: Analysis of precursors and successors, Monthly weather review, 118, 2056–2081, 1990.

Wiedenmann, J. M., Lupo, A. R., Mokhov, I. I., and Tikhonova, E. A.: The climatology of blocking anticyclones for the Northern and Southern Hemispheres: Block intensity as a diagnostic, Journal of climate, 15, 3459–3473, 2002.

Woollings, T., Barriopedro, D., Methven, J., Son, S.-W., Martius, O., Harvey, B., Sillmann, J., Lupo, A. R., and Seneviratne, S.: Blocking and its response to climate change, Current climate change reports, 4, 287–300, 2018.

Yamazaki, A. and Itoh, H.: Selective absorption mechanism for the maintenance of blocking, Geophysical research letters, 36, 2009.

Yamazaki, A. and Itoh, H.: Vortex–vortex interactions for the maintenance of blocking. Part I: The selective absorption mechanism and a case study, Journal of the Atmospheric Sciences, 70, 725–742, 2013a.

Yamazaki, A. and Itoh, H.: Vortex–vortex interactions for the maintenance of blocking. Part II: Numerical experiments, Journal of the Atmospheric Sciences, 70, 743–766, 2013b.

Zschenderlein, P., Pfahl, S., Wernli, H., and Fink, A. H.: A Lagrangian analysis of upper-tropospheric anticyclones associated with heat waves in Europe, Weather and Climate Dynamics, 1, 191–206, 2020.